LA-UR-25-24530

Approved for public release; distribution is unlimited.

Title: Hypercomplex Automatic Differentiation in the Eulerian Hydrocode PAGOSA

Author(s): Balcer, Matthew Ryan

Intended for: Report

Issued: 2025-05-09

Los Alamos
NATIONAL LABORATORY

Hypercomplex Automatic Differentiation in the Eulerian Hydrocode PAGOSA

Matthew Balcer[1]

[1]Los Alamos National Laboratory (XCP-8), Los Alamos, NM

April 30, 2025

Abstract

Enabling the computation of partial derivatives or sensitivities in production hydrocodes is beneficial for design, optimization, sensitivity analysis, and uncertainty quantification. Traditional finite difference approximations of these sensitivities are inefficient since convergence studies of the step size is required for each parameter of interest. For these reasons, HYPercomplex Automatic Differentiation (HYPAD) was implemented in the Eulerian hydrocode PAGOSA. HYPAD is analogous to forward-mode automatic differentiation except hypercomplex numbers (numbers with multiple imaginary parts) are used instead of dual numbers. Accurate partial derivatives can be computed of all state variables with respect to multiple input variables in a single run. The method was implemented using operator overloading to handle hypercomplex algebra. HYPAD was demonstrated and verified on Sod's shock tube problem to compute derivatives of the state variables with respect to a material parameter, initial conditions, and geometry.

1 Introduction

Partial derivatives or sensitivities are beneficial for design, optimization, sensitivity analysis, and uncertainty quantification [1, 2]. Gradients and Hessians are beginning to be implemented in some areas like finite element analysis [3, 4], computational fluid dynamics [5], and radiation transport [6, 7]. References [8, 9] have implemented forward- and reverse-mode AD; however, to the author's knowledge, they are not readily available today. For this reason, an Automatic Differentiation (AD) method called HYPercomplex Automatic Differentiation (HYPAD) was implemented in the Eulerian hydrocode PAGOSA.

HYPAD is analogous to forward-mode AD, except dual numbers are replaced with hypercomplex numbers. Hypercomplex numbers are imaginary numbers with multiple imaginary directions. Multicomplex, multidual, also known as hyper-dual, and Order Truncated Imaginary (OTI) numbers are examples of hypercomplex numbers [10, 11, 12]. In the context of AD, OTI numbers are the most computationally efficient option since no redundant computations are required, unlike multicomplex and multidual numbers.

In the HYPAD method, arbitrary-order partial derivatives of all state variables with respect to multiple variables can be computed in a single simulation run, unlike traditional forward-mode AD where a separate run is required for each variable of interest. When the problem contains many variables, on the order of 100 variables or greater, reverse-mode adjoint AD becomes more computationally efficient than HYPAD. Figure 1 graphically shows a comparison of the performance of HYPAD to forward-mode AD and adjoint-based AD as a function of the number of variables and number of outputs desired. All of these methods usually outperform finite difference approximations since a step-size convergence is required to find the optimal value of the derivative.

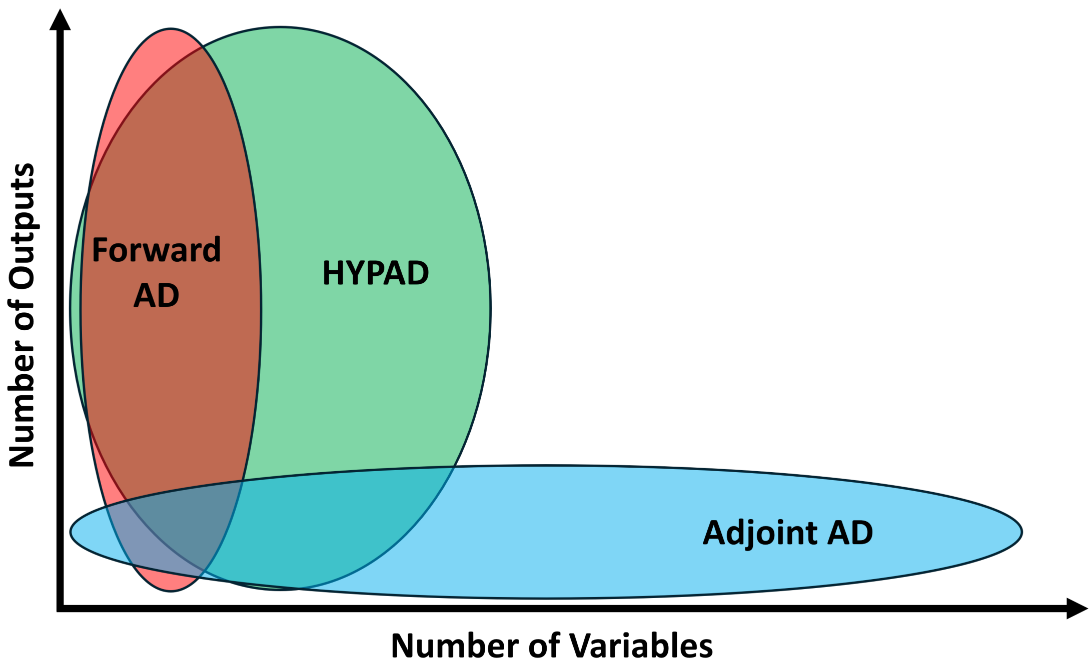

Figure 1: Comparison of HYPAD to forward-mode and adjoint-based AD as a function of number of variables and number of outputs

Higher-order derivatives can become intractable to compute with both forward-mode AD and adjoint-based AD since multiple passes are required. HYPAD with OTI numbers alleviates this burden by simply increasing the truncation order of the imaginary bases. The user can define the maximum derivative order desired prior to the analysis and the first- through n'th-order derivatives will be computed in a single run, in addition to the traditional output from the code [7].

2 Methodology

2.1 Central Difference Approximation

Central difference approximations of first-order partial derivatives are presented since they will be used to compare against HYPAD. The central difference approximation for first-order partial derivatives is

$$\frac{\partial f(x)}{\partial x} \approx \frac{f(x+h) - f(x-h)}{2h}, \tag{1}$$

where h is a step-size. This formula suffers from both subtraction cancellation error and truncation error. Therefore, a convergence study is required to find the optimal step-size that balances both of these errors.

2.2 Hypercomplex Automatic Differentiation (HYPAD)

Derivatives with respect to multiple variables of arbitrary-order may be computed using hypercomplex numbers, which have multiple non-real parts. Similar to forward-mode AD with dual numbers or finite difference, variables of interest are perturbed along unique non-real directions. The hypercomplex parts of the variables are propagated through the function evaluation and derivatives are extracted from the non-real parts of the outputs.

The most efficient hypercomplex number for HYPAD is Order Truncated Imaginary (OTI) numbers. An OTI number $c^* \in \mathbb{OTI}_d^n$ of d bases and truncation order n is represented by a real value and multiple non-real directions ϵ_i [12]. The OTI directions are analogous to multiple imaginary directions in multidual (or hyper-dual) numbers [11] except the imaginary bases are truncated above the expansion order n. That is, $\epsilon_1^{\alpha_1} \cdot \epsilon_2^{\alpha_2} \cdots \epsilon_d^{\alpha_d} = 0$, when the multiplicity of the OTI imaginary directions, $|\alpha| = \alpha_1 + \cdots + \alpha_d$, is $|\alpha| > n$. Using multi-index notation, an OTI number is represented by

$$c^* = \sum_{|\alpha|=0}^{n} \frac{1}{\alpha!} \boldsymbol{\epsilon}^{\alpha} \partial^{\alpha} f\left(\boldsymbol{x}_0\right), \; c^* \in \mathbb{OTI}_d^n, \tag{2}$$

where $\boldsymbol{x}_0 = [x_{1_0}, ..., x_{d_0}] \in \mathbb{R}^d$ is a vector of constants at which the derivative $\partial^{\alpha} f\left(\boldsymbol{x}_0\right) = \frac{\partial^{\alpha} f(\boldsymbol{x}_0)}{\partial x_1^{\alpha_1} \cdots \partial x_d^{\alpha_d}}$, $\boldsymbol{\epsilon} = [\epsilon_1, ..., \epsilon_d]$ is a vector of OTI imaginary directions of size d, and

$$\boldsymbol{\epsilon}^{\alpha} = \prod_{s=1}^{d} \epsilon_s^{\alpha_s}. \tag{3}$$

OTI numbers have the same structure as the Taylor series expansion of order n and d variables. Partial derivatives are extracted from an OTI number by

$$\partial^{\alpha} f\left(\boldsymbol{x}_0\right) = \alpha! \cdot \mathrm{Im}_{\alpha}[c^*]. \tag{4}$$

2.3 Implementation of HYPAD in PAGOSA

HYPAD can be implemented in code by converting variables of interest, and variables that depend on these variables, from real variables to hypercomplex variables. An external FORTRAN library was linked to PAGOSA so that algebraic operations are overloaded with hypercomplex algebra. The library used in this work is called OTILib [12]. OTILib is open-source and available on GitHub at https://github.com/mauriaristi/otilib. The current version of the FORTRAN OTILib requires the number of bases and order of bases to be defined before the analysis. This means, different versions of OTILib need to be used based on the order of derivative and number of variables of interest for the particular analysis.

Several other modifications to the source code were performed. Boolean logic statements such as if and while statements need to be based on the real part of the variables. That is, the real part of all hypercomplex variables was used in boolean statements. Intrinsic FORTRAN functions, such as MAX, MIN, MAXLOC, MINLOC, etc. do not support hypercomplex variables. So, custom functions were implemented to base these functions on the real part of the complex variables, and the function returns the real part with the corresponding imaginary part.

3 Numerical Example: Sod's Shock Tube Problem

Consider a shock tube with a rectangular cross-section with two materials separated by a diaphragm, which is modeled as a discontinuity, at the center of the tube [13]. When the diaphragm is removed, a shock wave propagates through the tube. The initial density, velocity, pressure, and specific energy of the two materials are

$$(\rho,\, u,\, P,\, e) = \begin{cases} (1.0,\ 0,\ 1.0,\ 2.5), & x \leq 50 \text{ cm}, \\ (0.125,\ 0,\ 0.1,\ 2.0), & x > 50 \text{ cm}. \end{cases} \tag{5}$$

In PAGOSA, the initial pressure is computed from the initial energy and density from the Equation Of State (EOS). The ideal gas EOS was used to model both materials, which is defined as

$$P = (\gamma - 1)e\rho \tag{6}$$

and the squared sound speed is computed as

$$c^2 = \gamma(\gamma - 1)e. \tag{7}$$

A two-dimensional (2D) geometry was used to model the shock tube where the domain of the tube in the (x, y) directions was $x \in [0, 100 \text{ cm}]$, $y \in [-5, 5 \text{ cm}]$, respectively. The mesh was spatially discretized in the (x, y) directions as $N_x = 200$, $N_y = 20$, respectively, to obtain a 5 mm mesh resolution and the maximum time was $t_{\max} = 0.2$ s. The cell width in the x-direction was used as the artificial viscosity indicator. All other variables were set at the PAGOSA default parameters. The input file used for this simulation is shown in Appendix A.

First-order partial derivatives of the state variables (density, the x component of velocity, pressure, and specific energy, and sound speed) with respect to the variables shown in Table 1 were computed with HYPAD at every vertex in the mesh and at every time step. Table 1 also shows the OTI directions that each variable was perturbed along. The initial conditions were perturbed with a value of one along ϵ_i for $x \leq 50$ cm for the left material and $x > 50$ cm for the right material. γ was perturbed along the ϵ_5 direction with a value of one. Derivatives of the diaphragm location x_d were computed by perturbing the vertex coordinates in the x-direction along the ϵ_6 direction with the following magnitude

$$f(x) = \begin{cases} 1 & \text{if } x = 0.5l \\ \frac{x - 0.45l}{0.05l} & \text{else if } 0.45l < x < 0.5l \\ \frac{0.55l - x}{0.05l} & \text{else if } 0.5l < x < 0.55l \\ 0 & \text{otherwise} \end{cases} \tag{8}$$

where $l = 100$ cm is the length of the shock tube. The magnitude of the perturbation applied to the coordinates scales linearly from 0 to 1 on 5% of the mesh on the left side of the diaphragm. Similarly, coordinates scale linearly from 1 to 0 on 5% of the mesh on the right side of the diaphragm. This creates a smooth perturbation around the diaphragm.

The version of OTILib used for this example was optimized to handle OTI numbers of order $n = 1$ and truncation order $m = 6$, so that first-order derivatives of all six variables can be computed in the same run. The HYPAD method was compared to central difference of the as-is PAGOSA version 17.4.9 simulation [14] and central difference of the analytic solution [13]. Perturbations in the central difference approximations with PAGOSA were applied in the input file so that source-code was not modified.

Table 1: Variables of Interest for Sod's Shock Tube Problem

Type	Variable	Symbol	Value	Units	Basis
Initial Condition	Initial density of left material	ρ_{0L}	1.0	g cm^{-3}	ϵ_1
	Initial density of right material	ρ_{0R}	0.125	g cm^{-3}	ϵ_2
	Initial energy of left material	e_{0L}	2.5	Mbar cm^3 g^{-1}	ϵ_3
	Initial energy of right material	e_{0R}	2.0	Mbar cm^3 g^{-1}	ϵ_4
Material Parameter	Adiabatic constant of both materials	γ	1.4	-	ϵ_5
Geometry	Diaphragm location	x_d	50	cm	ϵ_6

3.1 Real Values

The real values of the output from a HYPAD simulation should be identical to the output from a traditional simulation. Figure 2 shows the real values of the state variables of the HYPAD simulation compared to a traditional PAGOSA simulation and the analytical solution. There is some discrepancy between HYPAD and traditional PAGOSA near the shock boundaries, which is most noticeable in e and c. The HYPAD implementation is currently being assessed to identify the cause of this discrepancy.

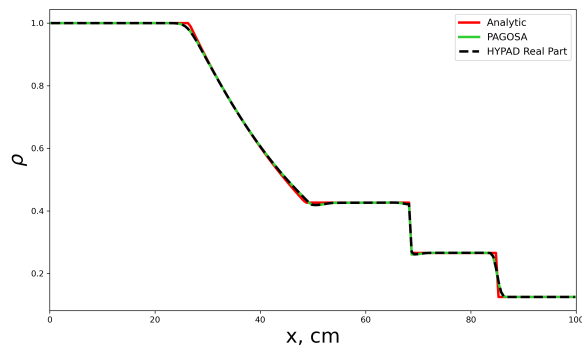

(a) Density, ρ

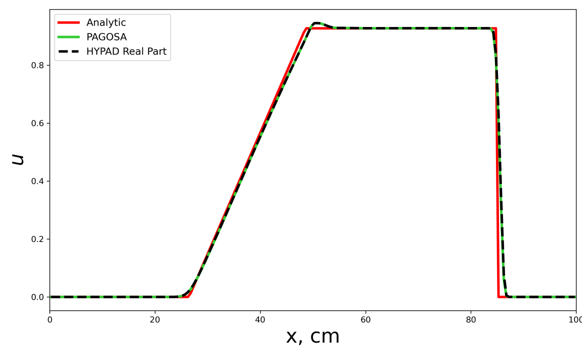

(b) x-Component of Velocity, u

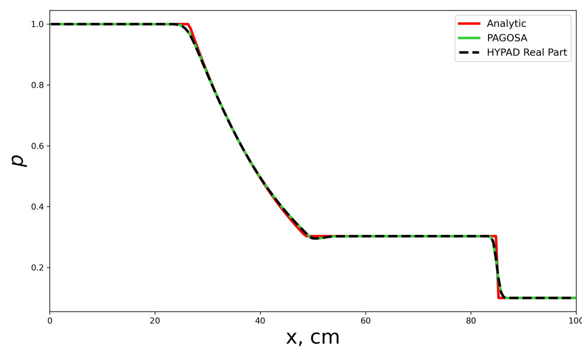

(c) Pressure, p

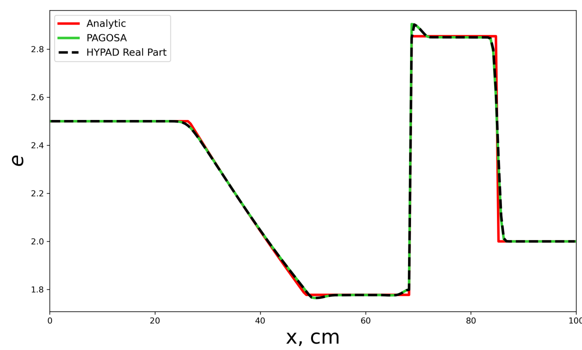

(d) Specific Energy, e

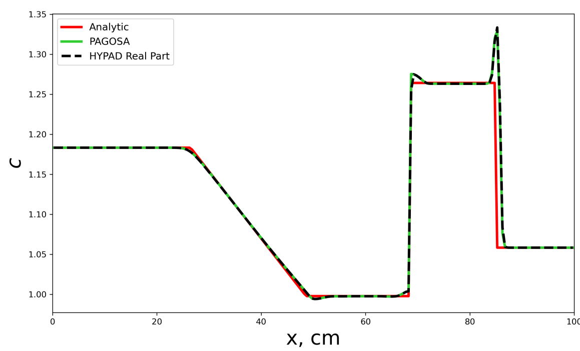

(e) Sound Speed, c

Figure 2: State variables at $t = 20$ ms. Analytic solution compared to standard PAGOSA and the real part of HYPAD.

3.2 First-order Partial Derivatives of State Variables

First-order partial derivatives of the state variables were computed with HYPAD. Figures 3 through 7 show HYPAD derivatives compared to central difference of the analytic solution and central difference of a traditional PAGOSA simulation. HYPAD derivatives are as good or better than central difference compared to central difference of the analytic solution for initial conditions and material parameters. However, the geometric derivative is worse than the central difference of PAGOSA. A convergence study may be conducted on the percentage of mesh that is perturbed to find a superior perturbation method. A convergence study can also be conducted on the resolution of the Eulerian mesh.

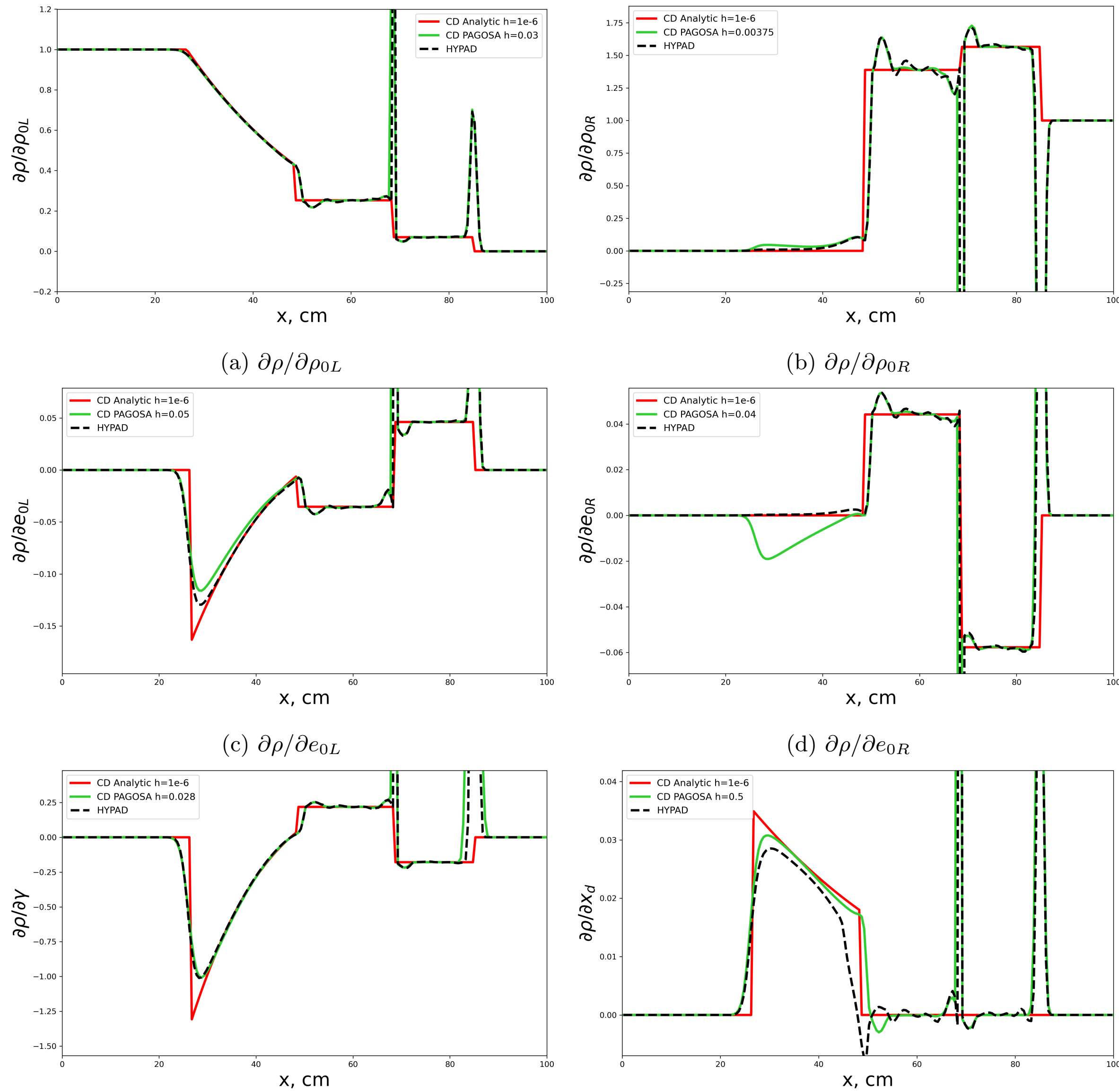

(a) $\partial\rho/\partial\rho_{0L}$ (b) $\partial\rho/\partial\rho_{0R}$

(c) $\partial\rho/\partial e_{0L}$ (d) $\partial\rho/\partial e_{0R}$

(e) $\partial\rho/\partial\gamma$ (f) $\partial\rho/\partial x_d$

Figure 3: HYPAD-based first-order partial derivatives of density with respect to each input variable compared to analytic and central difference approximations. 'CD Analytic' is central difference of the analytic solution with step-size h. 'CD PAGOSA' is central difference of PAGOSA with step-size h.

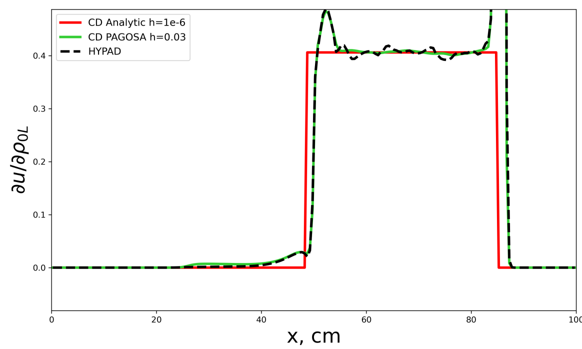

(a) $\partial u/\partial \rho_{0L}$

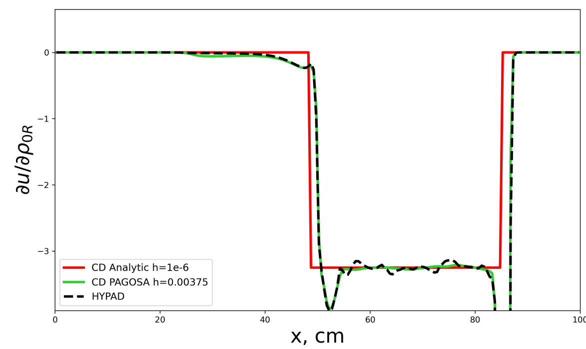

(b) $\partial u/\partial \rho_{0R}$

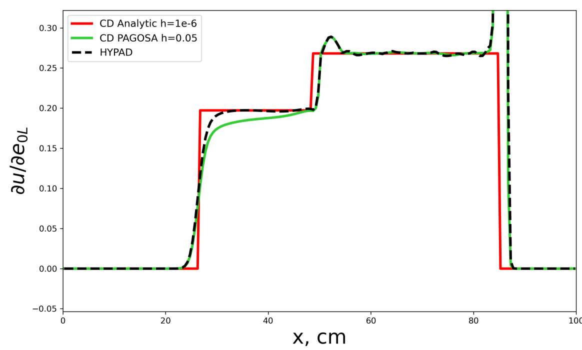

(c) $\partial u/\partial e_{0L}$

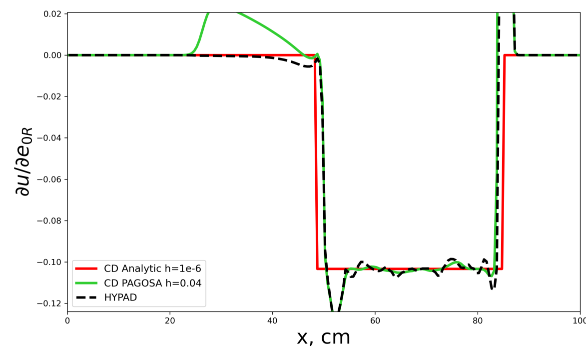

(d) $\partial u/\partial e_{0R}$

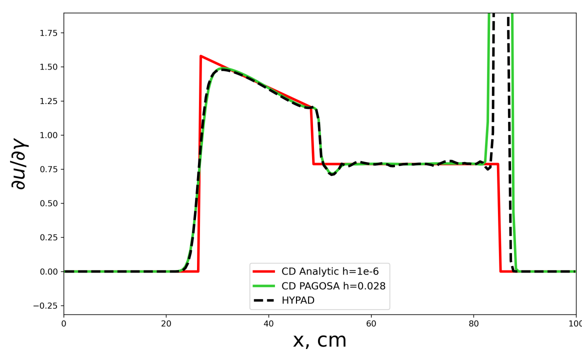

(e) $\partial u/\partial \gamma$

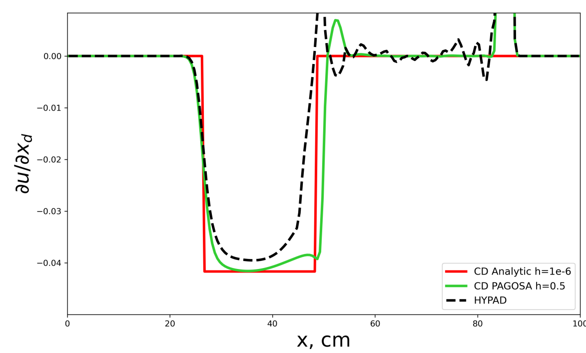

(f) $\partial u/\partial x_d$

Figure 4: HYPAD-based first-order partial derivatives of velocity with respect to each input variable compared to analytic and central difference approximations. 'CD Analytic' is central difference of the analytic solution with step-size h. 'CD PAGOSA' is central difference of PAGOSA with step-size h.

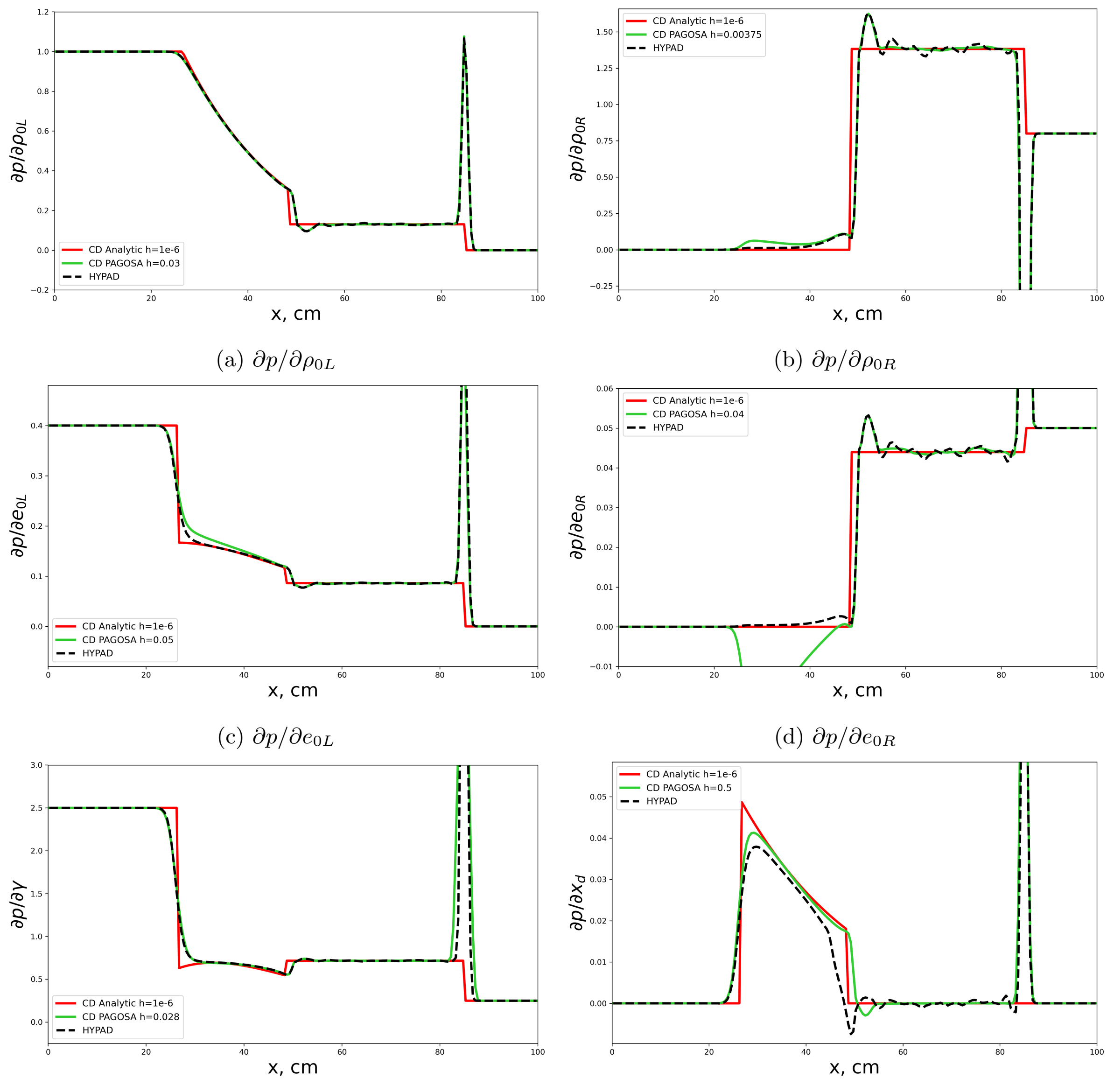

(a) $\partial p/\partial \rho_{0L}$ (b) $\partial p/\partial \rho_{0R}$

(c) $\partial p/\partial e_{0L}$ (d) $\partial p/\partial e_{0R}$

(e) $\partial p/\partial \gamma$ (f) $\partial p/\partial x_d$

Figure 5: HYPAD-based first-order partial derivatives of pressure with respect to each input variable compared to analytic and central difference approximations. 'CD Analytic' is central difference of the analytic solution with step-size h. 'CD PAGOSA' is central difference of PAGOSA with step-size h.

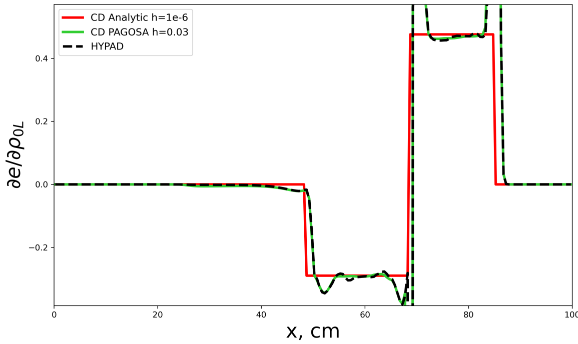

(a) $\partial e/\partial \rho_{0L}$

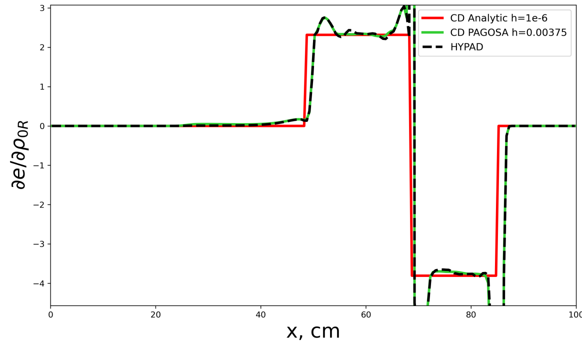

(b) $\partial e/\partial \rho_{0R}$

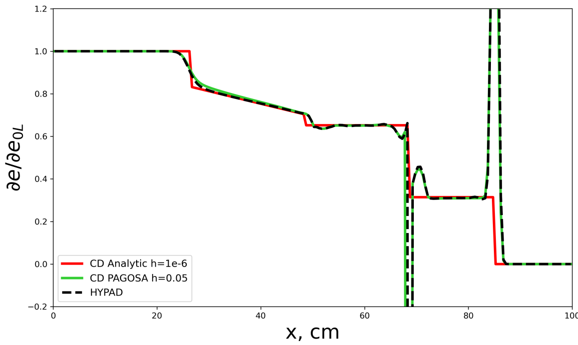

(c) $\partial e/\partial e_{0L}$

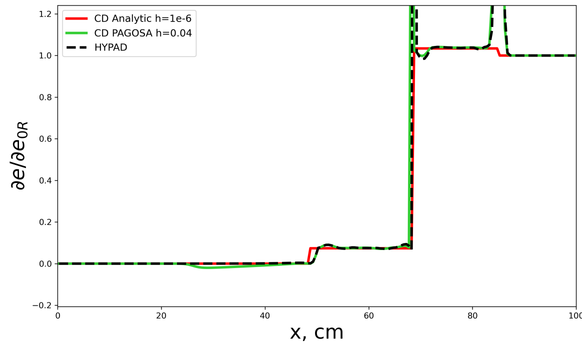

(d) $\partial e/\partial e_{0R}$

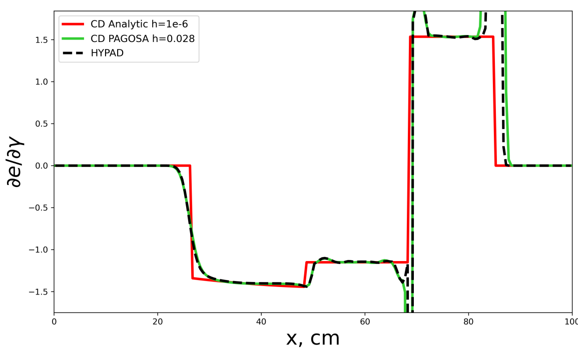

(e) $\partial e/\partial \gamma$

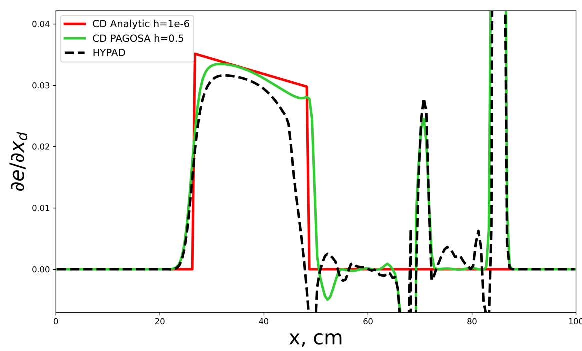

(f) $\partial e/\partial x_d$

Figure 6: HYPAD-based first-order partial derivatives of specific energy with respect to each input variable compared to analytic and central difference approximations. 'CD Analytic' is central difference of the analytic solution with step-size h. 'CD PAGOSA' is central difference of PAGOSA with step-size h.

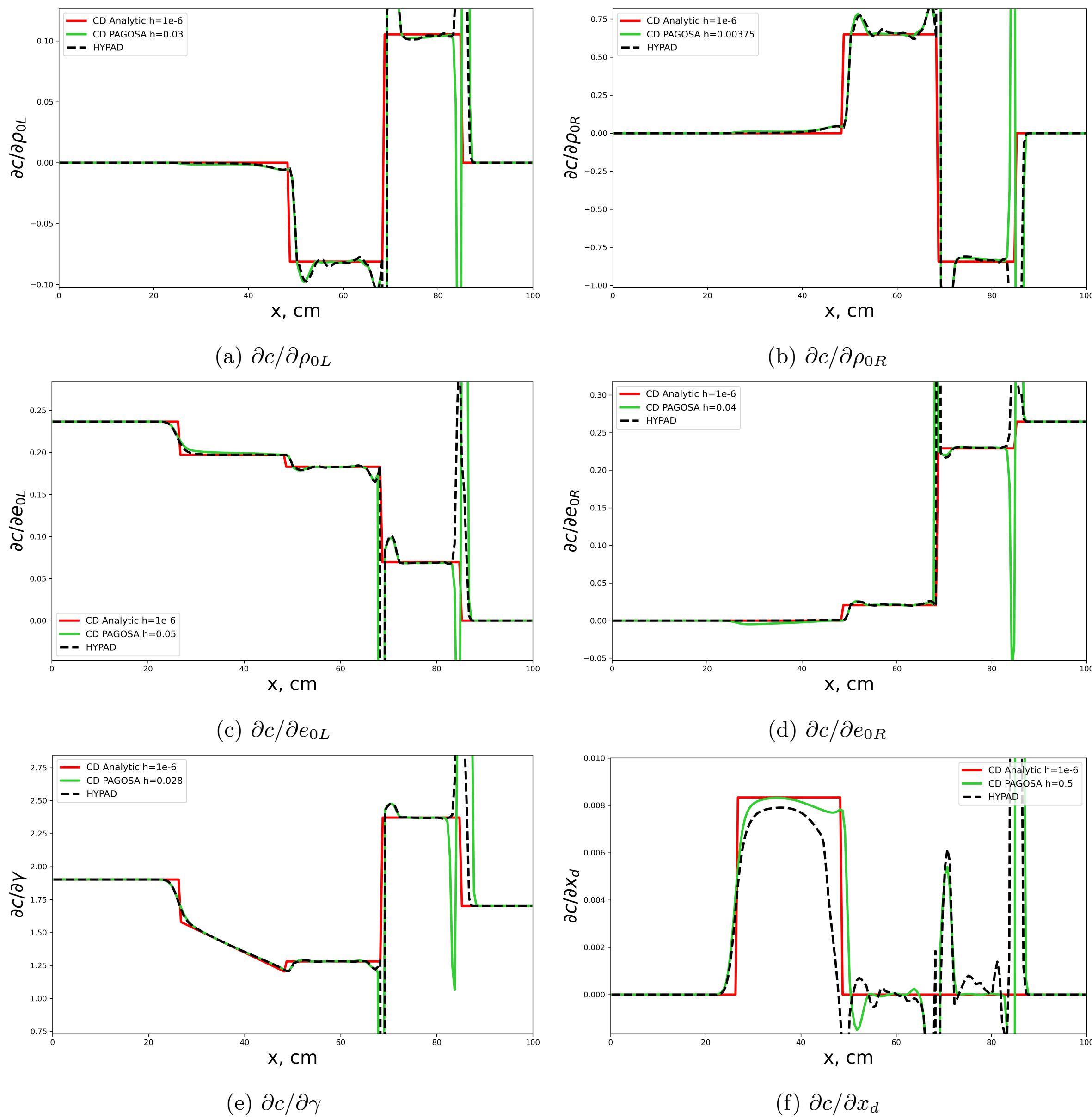

(a) $\partial c/\partial \rho_{0L}$ (b) $\partial c/\partial \rho_{0R}$

(c) $\partial c/\partial e_{0L}$ (d) $\partial c/\partial e_{0R}$

(e) $\partial c/\partial \gamma$ (f) $\partial c/\partial x_d$

Figure 7: HYPAD-based first-order partial derivatives of sound speed with respect to each input variable compared to analytic and central difference approximations. 'CD Analytic' is central difference of the analytic solution with step-size h. 'CD PAGOSA' is central difference of PAGOSA with step-size h.

4 Discussion

Shock boundaries are numerical discontinuities, which result in large derivative values in regions around the shock front. PAGOSA attempts to smooth these discontinuities using an artificial viscosity term. Smoothing techniques such as window filtering may be applied to the derivatives to reduce the spikes in the derivative values near these shock fronts and oscillations [15].

Oscillations near shock fronts are also produced by PAGOSA's smoothing method. The effect of these oscillations are amplified in the derivatives.This effect will increase with order of derivative. Smoothing methods like window filtering may help reduce these non-physical oscillations.

5 Summary and Future Work

This work implemented HYPercomplex Automatic Differentiation (HYPAD) in the Eulerian hydrocode PAGOSA. To the author's knowledge, this is the first time hypercomplex differentiation was proven to work in hydrocode simulations. The method was verified on Sod's shock tube problem in a two-dimensional cartesian simulation. Partial derivatives of all state variables (density, pressure, velocity, specific energy, and sound speed) with respect to six variables including initial conditions, a material parameter, and geometry, were computed in a single simulation. HYPAD agreed well with central difference of PAGOSA and central difference of the analytic solution.

HYPAD allows second- and higher-order partial derivatives to be computed in a straight-forward manner (increasing truncation order of the OTI algebra). Therefore, future work will compute and verify higher-order derivatives with HYPAD. Future work will also include implementation of additional physics including burn, strength, fracture, and crush physics in PAGOSA.

References

[1] J. R. Martins and A. Ning. *Engineering design optimization.* Cambridge University Press, 2021. ISBN: 9781108833417.

[2] M. Balcer, M. Aristizibal, J. Rincon Tabares, A. Montoya, D. Restrepo, and H. Millwater. "Hypad-uq: a derivative-based uncertainty quantification method using a hypercomplex finite element method". *J. Verif. Valid. Uncert.* (2023), pp. 1–45. DOI: 10.1115/1.4062459.

[3] J.-S. Rincon-Tabares, M. Aristizabal, M. Balcer, A. Montoya, H. Millwater, and D. Restrepo. "Efficient sensitivity analysis of the thermal profile in powder bed fusion of metals using hypercomplex automatic differentiation finite element method". *Additive Manufacturing* 94 (2024), p. 104488. ISSN: 2214-8604. DOI: 10.1016/j.addma.2024.104488. URL: https://www.sciencedirect.com/science/article/pii/S2214860424005347.

[4] A. M. Aguirre-Mesa, D. Ramirez-Tamayo, M. J. Garcia, A. Montoya, and H. Millwater. "A stiffness derivative local hypercomplex-variable finite element method for computing the energy release rate". *Eng. Fract. Mech.* 218 (Sept. 2019), p. 106581. ISSN: 0013-7944. DOI: 10.1016/j.engfracmech.2019.106581.

[5] J. R. Martins, J. J. Alonso, and J. J. Reuther. "A Coupled-Adjoint Sensitivity Analysis Method for High-Fidelity Aero-Structural Design". *Optimization and Engineering* 6.1 (Mar. 2005), pp. 33–62. ISSN: 1573-2924. DOI: 10.1023/B:OPTE.0000048536.47956.62. URL: https://doi.org/10.1023/B:OPTE.0000048536.47956.62.

[6] J. A. Favorite and T. Burr. "Second-order uncertainty analysis for radiation shielding problems using mcnp". *Trans. Am. Nucl. Soc.* 116 (2017), pp. 595–598. ISSN: 0003-018X. URL: https://inis.iaea.org/search/search.aspx?orig_q=RN:52087876.

[7] M. R. Balcer, H. Millwater, and J. A. Favorite. "Multidual sensitivity method in ray-tracing transport simulations". *Nucl. Sci. Eng.* 195.9 (Sept. 2021), pp. 907–936. ISSN: 0029-5639. DOI: 10.1080/00295639.2021.1883949.

[8] M. L. Rightley, R. J. Henninger, and K. M. Hanson. "Adjoint differentiation of hydrodynamic codes". *CNLS Research Highlights* (1998).

[9] R. J. Henninger, A. Carle, and P. J. Maudlin. "Hydrocode sensitivities by means of automatic differentiation". eng. *Scientific and technical aerospace reports* 39 (2001). ISSN: 1548-8837.

[10] G. Lantoine, R. P. Russell, and T. Dargent. "Using multicomplex variables for automatic computation of high-order derivatives". *ACM Transactions on Mathematical Software* 38.3 (2012), pp. 1–21. ISSN: 0098-3500. DOI: 10.1145/2168773.2168774.

[11] J. A. Fike and J. J. Alonso. "The development of hyper-dual numbers for exact second-derivative calculations". *49th aiaa aerospace sciences meeting including the new horizons forum and aerospace exposition* (Orlando, Florida). American Institute of Aeronautics and Astronautics, Jan. 2011, pp. 886–903. DOI: 10.2514/6.2011-886.

[12] M. Aristizabal Cano. "Order truncated imaginary algebra for computation of multivariable high-order derivatives in finite element analysis". PhD thesis. Universidad EAFIT, 2020.

[13] G. A. Sod. "A survey of several finite difference methods for systems of nonlinear hyperbolic conservation laws". *Journal of Computational Physics* 27.1 (1978), pp. 1–31. DOI: 10.1016/0021-9991(78)90023-2.

[14] W. N. Weseloh, S. P. Clancy, and J. W. Painter. *PAGOSA physics manual*. Tech. rep. LA-14425-M. Los Alamos National Laboratory (LANL), Los Alamos, NM (United States), 2010.

[15] M. Balcer, M. Aristizabal, J.-S. RinconTabares, A. Montoya, D. Restrepo, and H. Millwater. "Uncertainty Quantification of High-Dimensional Additive Manufacturing Simulations using Non-Intrusive Hypercomplex Automatic Differentiation". *Los Alamos National Laboratory* LA-UR-25-23915 (draft) (2025).